Sensors and Actuators B 238 (2017) 374–380

Contents lists available at ScienceDirect

Sensors and Actuators B: Chemical

journal homepage: www.elsevier.com/locate/snb

Optimization of metal nanoparticle amount on SnO_2 nanowires to achieve superior gas sensing properties

Zain Ul Abideen, Jae-Hun Kim, Sang Sub Kim *

Department of Materials Science and Engineering, Inha University, Incheon 402-751, Republic of Korea

ARTICLE INFO

Article history:
Received 29 March 2016
Received in revised form 5 July 2016
Accepted 13 July 2016
Available online 14 July 2016

Keywords:
Gas sensing
Functionalization
Nanowire
SnO_2
Ag
Sensitization

ABSTRACT

SnO_2 nanowires (NWs) functionalized with Ag nanoparticles (NPs) were tested for NO_2 gas sensing ability; the results revealed a bell-shaped curve as a function of the surface coverage of Ag NPs. A model that can explain these experimental observations regarding the functionalization of metal NPs on oxide NWs, which is the most widely used approach for improving the sensing capabilities of NWs, was proposed and validated. Based on the electronic and chemical sensitizations of metal NPs, a mathematical equation was formulated to predict the optimal surface coverage of metal NPs on the NWs to obtain maximum sensing performance. This study may provide new insight and guidelines for the development of highly sensitive NW-based gas sensors.

1. Introduction

In recent years, the detection of toxic gases in modern industrial environments has become an important area of study. Considerable effort has been made to realize highly sensitive and selective chemical gas sensors, including the creative design of new materials and sensor structures. The use of nanostructured materials including nanowires (NWs) is one of the most efficient routes for achieving sensitive chemical sensors owing to their favorable surface to bulk ratio, good crystallinity, fast diffusion kinetics, and self-heating effects [1–6].

Functionalization (or decoration) with metal nanoparticles (NPs) has long been used to further improve the sensing abilities of oxide NWs [7–9]. Electronic and/or chemical sensitizations are considered responsible for the improvement. Noble metal elements including Pd, Pt, Au, and Ag (which act as sensitizers or catalysts) are attached in the form of NPs to the surface of NWs using a range of methods, such as photochemistry [10], reverse micelles [11], arc discharge [12], sonochemistry [13], γ-ray radiolysis [14,15], and vacuum deposition [16]. The sensing properties of the hybrid system are affected by the amount of functionalized metal NPs. A generally observed trend in the sensitivity of metal NP-functionalized NWs is a bell-shaped curve as a function of the NP amount. Recently, Ding et al. [17] and Hwang et al. [18] investigated the sensing properties of ZnO and SnO_2 nanomaterials, respectively, decorated with Ag NPs. They observed deteriorations in the gas response after a certain amount of Ag particles, emphasizing the need to optimize the amount of functionalized metal NPs. Although the functionalization process is generally accepted to be an effective route to upgrading the sensing properties of NWs, to the best of our knowledge, there are only a few reports of optimizing the functionalization in terms of the amount of metal NPs on NWs.

In this work, the NO_2-sensing characteristics of Ag-functionalized SnO_2 NWs are experimentally investigated as a function of the surface coverage of Ag NPs. We then propose a model for explaining the surface coverage-dependent sensing performances, which can be used as a guideline for achieving optimized performance of oxide NWs when functionalized by metal NPs.

2. Experimental

In this work, as a model experiment, SnO_2 NWs functionalized with Ag NPs were tested for NO_2 gas sensing. For the sensor platform, SnO_2 NWs were grown in a network on patterned interdigital electrode (IDE) pads using the well-known vapor–liquid–solid method. Because the experimental procedure for fabricating SnO_2 NWs sensors is described in detail in earlier reports [8,19,20], only a brief explanation is included here. Firstly, IDEs were made on

* Corresponding author.
E-mail addresses: sangsub@inha.ac.kr, sangsub99@gmail.com (S.S. Kim).

http://dx.doi.org/10.1016/j.snb.2016.07.054
0925-4005/

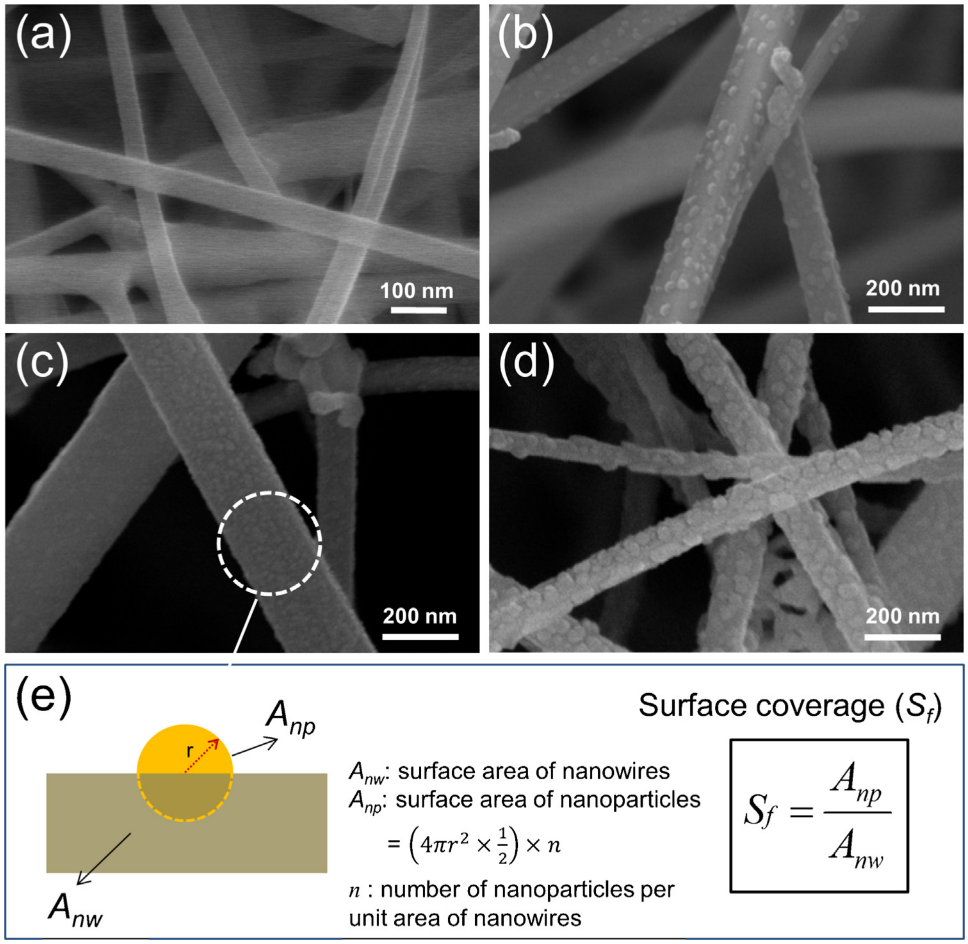

Fig. 1. Microstructures of SnO_2 NWs functionalized with varying amounts of Ag NPs: (a) S_f = 0, (b) S_f = 0.73, (c) S_f = 0.88 and (d) S_f = 1.76. (e) A schematic illustration describing S_f.

SiO_2-grown Si (100) substrates using a conventional photolithographic process. A tri-layer electrode consisting of Au (3 nm)/Pt (100 nm)/Ti (100 nm) was sequentially deposited by a sputtering method. The Au top layer served as a catalytic layer for the selective growth of SnO_2 NWs. The substrate on which the IDEs had been prepared was introduced into a horizontal quartz tube furnace, in which an alumina crucible containing Sn powder was also placed. The furnace was then heated to 900 °C for 15 min while flowing N_2 and O_2 at rates of 300 and 10 sccm/min, respectively. The SnO_2 NWs grown on the IDEs became tangled with each other, producing chemiresistive electrical transport channels.

γ-ray radiolysis was employed to functionalize the Ag NPs on the SnO_2 NWs. The precursor solution for the γ-ray radiolysis was prepared by the following procedure. 2×10^{-3} concentration of silver nitrate ($AgNO_3$, Sigma-Aldrich) was dissolved in a mixture of deionized water (90 vol%) and 2-propanol (10 vol%). The mixed solution was stirred for 24 h. The fabricated networked SnO_2 NWs sensors were immersed in the solution, subsequently illuminated with ^{60}Co γ-rays at the Korea Atomic Energy Research Institute. After the γ-ray illumination, the sensor samples were taken from the solution and heat treated at 500 °C for 1 h in air. Earlier reports by the present authors demonstrated that this technique is an effective route to synthesize various kinds of metal NPs on NWs in a controlled manner [8,21,22]. The γ-ray radiolysis conditions used in this work were as follows: exposure time: 1–4 h at 10 kGy h^{-1} and 2×10^{-3} mM $AgNO_3$; dose rate: 2–15 kGy h^{-1} at 2×10^{-3} mM $AgNO_3$ for 3 h.

The NO_2-sensing behavior of the Ag-functionalized SnO_2 NWs was measured using a gas sensing system. In our earlier report [8], the Ag functionalization was found to greatly enhance the response and selectivity of the SnO_2 NWs for detecting NO_2. The high selectivity and sensitivity of the Ag-functionalized SnO_2 NWs was attributed to the particular energy-band structure of the surface of the SnO_2 NWs functionalized by the Ag NPs, as well as the catalytic role of Ag in dissociating NO_2 into more active chemical species. Therefore, as a model experiment, the NO_2-sensing behavior was investigated with respect to the surface coverage, namely the amount, of Ag NPs. The sensor response (S) was estimated as $S = R_g/R_a$ where R_a and R_g are the resistances in the absence and presence of NO_2, respectively. The gas concentration was controlled by changing the mixing ratio of the target gas (NO_2) to dry air through mass flow controllers. The operating temperature was 300 °C, which was selected after preliminary screening experiments [8]. The microstructure of the sensors was examined by field-emission scanning electron microscopy (FE-SEM, Hitachi, S-4200). Other material properties of the sensors, including phase and crystallinity, were the same as those previously reported [8].

3. Results and discussion

3.1. SnO_2 NWs functionalized with Ag NPs

Microstructures of the SnO_2 NWs with varying amount of Ag NPs are shown in Fig. 1. For the purpose of quantifying the amount of Ag NPs on SnO_2 NWs, the surface coverage (S_f) was used. S_f is defined as the ratio of the average surface area (A_{np}) of Ag NPs to the unit surface area (A_{nw}) of SnO_2 NWs. A_{np} was calculated from

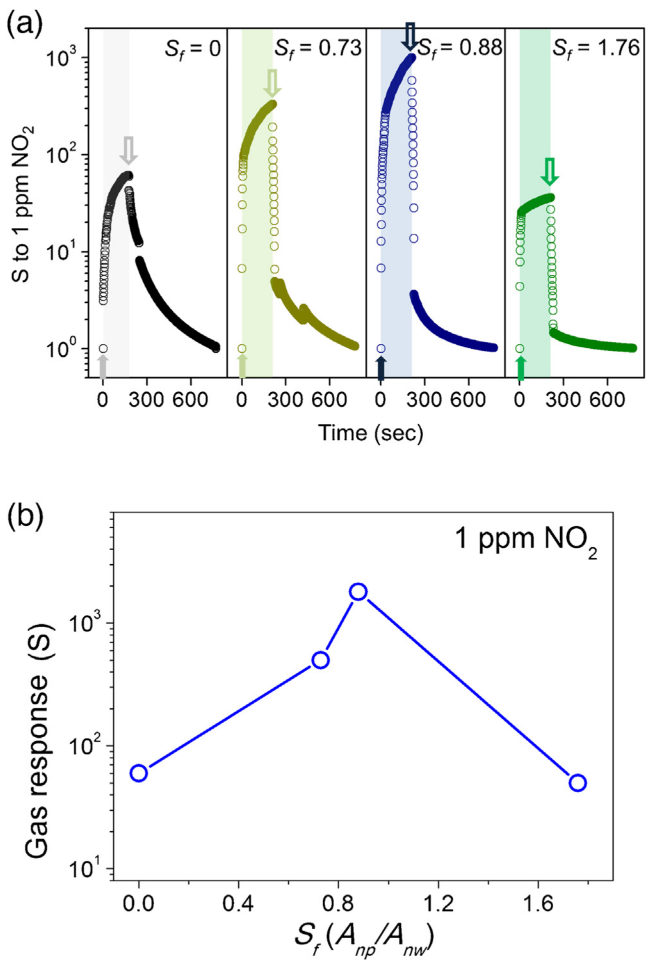

Fig. 2. (a) Response curves and (b) summary of the responses of SnO_2 NWs functionalized with Ag NPs as a function of S_f.

the average size and formation density of the NPs, assuming that the shape of the NPs is hemispherical. Fig. 1e shows a schematic illustration of how S_f is calculated, where the calculated S_f values are denoted in the figure. In particular, Fig. 1a shows uncoated SnO_2 NWs with zero S_f.

The response curves to 1 ppm NO_2 of the SnO_2 NWs functionalized with surface coverage of Ag NPs in the range of 0–1.76 are shown in Fig. 2a. The response is plotted as a function of S_f in Fig. 2b. It can be seen that the response greatly improves between $S_f = 0$ and $S_f = 0.88$. However, a further increase to $S_f = 1.76$ severely deteriorates the response. This bell-shaped gas response as a function of S_f suggests that optimization of S_f is a key control parameter in metal NP–functionalized oxide NWs sensors. The improvement in the sensing behavior by the functionalization with Ag NPs is caused by the combination of electronic and chemical sensitizations. It is noteworthy that the gas response curve of SnO_2 NWs with $S_f = 1.76$ saturated much faster than NWs with smaller loads. The relatively shorter distance between functionalized NPs can allow the arriving gas molecules to be transferred more quickly to the surface of the NWs. This is a case where a larger amount of surface decoration, namely higher S_f, is possibly responsible for the fast response and recovery times.

In the electronic sensitization (ES), NPs act as a donor or acceptor of electrons from the oxide. During such interaction between metal and semiconductor, a change in the surface conductivity of the semiconductor may occur due to the change in the electrical state of the metal particles upon interaction with the target gas [23,24]. This type of sensitization has so far been observed for SnO_2 sensors loaded with Ag, Pd, or Cu. Direct evidences supporting the electrical interactions between SnO_2 and Ag_2O have been obtained by X-ray photoelectron spectroscopy (XPS) [24,25]. In contrast, for chemical sensitization (CS), gas molecules are activated by the metal NPs and are spilt-over to the oxide surface to facilitate the chemical reaction of the gas molecules on the semiconductor [23]. The spillover phenomenon is known to occur in metal NP-functionalized oxide nanowires [26]. In this work, a general model is derived considering both sensitization mechanisms and we further explain their role in the total sensitization of the NWs. The model can be used as a guideline for functionalizing oxide NWs sensors with metal NPs.

3.2. Model formulation for functionalization of oxide NWs with metal NPs

The functionalization of NWs with metal NPs results in an improvement in the sensing performance of NWs due to two effects: ES and CS. Despite the clear effect of metal NPs observed experimentally, it is unclear why these sensitizations lead to a pronounced difference in the resistance of NWs during the various interactions with the gas molecules. Here, we explain with a simple geometric approach why a larger effect on the resistance occurs when metal NPs are attached to NWs.

The gas response (S) of any n-type sensor material for oxidizing gases is defined as follows:

$$S = \frac{R_g - R_a}{R_a} = \frac{R_g}{R_a} - 1 = \frac{\Delta R}{R_a}, \quad R_g > R_a \tag{1}$$

where R_g is the resistance in the presence and R_a is the resistance in the absence of the target gas.

The resistance R of a NW with length l and cross-sectional area A of the conduction channel can be described as follows:

$$R = \rho \frac{l}{A} \tag{2}$$

where ρ is the resistivity in the conduction channel of the NW.

Considering the change in the area of the conduction channel and neglecting the small, but existing, current in the depletion region, Eq. (3) can be used to describe pure n-type NWs with circular cross-sectional areas in the presence of an oxidizing gas, as follows:

$$S_p = \frac{\rho \frac{l}{A_g} - \rho \frac{l}{A_a}}{\rho \frac{l}{A_a}} = \frac{A_a - A_g}{A_g} = \frac{\Delta A_c}{A_g} \tag{3}$$

Here S_p is the gas response of pure n-type NWs without functionalization, A_a is the cross-sectional area of the conduction channel in the absence, and A_g is the cross-sectional area of the conduction channel in the presence of the target gas, and ΔA_c is the difference in the area of the conduction channel between the two cases.

The above-mentioned approach is illustrated schematically in Fig. 3a. In contrast, stronger resistance modulation is present due to ES when metal NPs are attached to NWs, as shown schematically in Fig. 3b. To simplify the model, the transducer effect that is well known as the Schottky depletion layer model [27,28] is included in the ES effect. This is appropriate, as the transducer effect is dependent on the interface area formed between NPs and NWs, in which the conduction channel in the NW is suppressed by the electron flow from the NW to the metal NP. In this case, Eq. (3) can be modified and generalized for oxidizing gases as follows:

$$S_e = \left(\frac{\Delta A_c}{A_g}\right)_f \tag{4}$$

Here, S_e is the gas response of the functionalized n-type NWs solely considering ES, the subscript f represents the case of functionalized

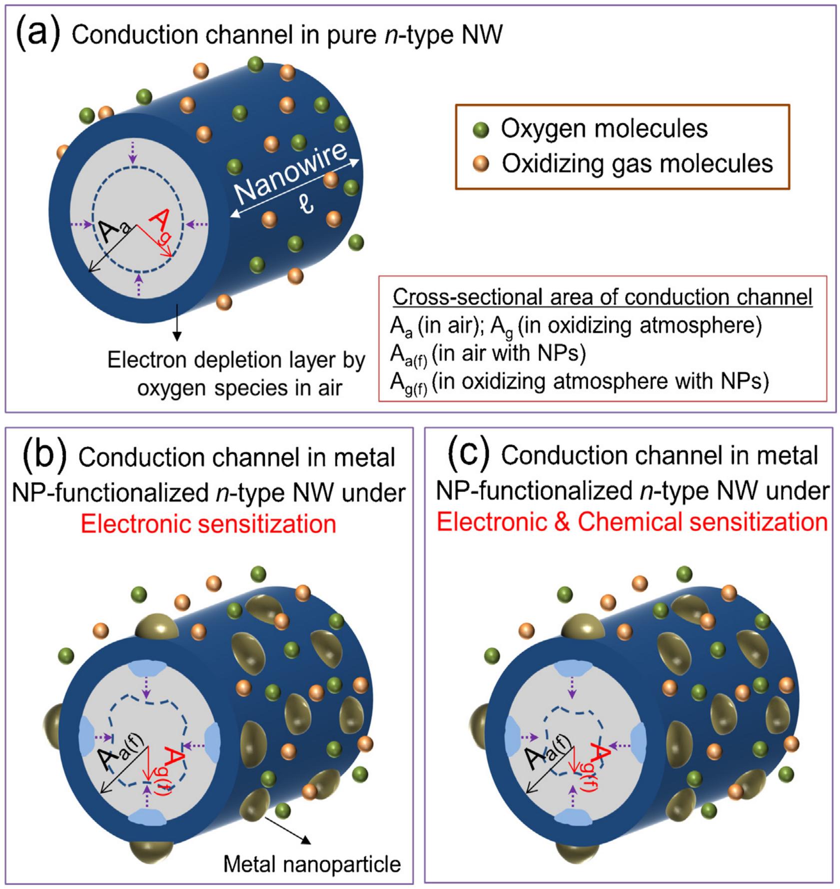

Fig. 3. Schematic diagram showing the intensified resistance modulation of NWs due to the functionalization with metal NPs. Changes in conduction channel by oxidizing gas molecules for (a) pure *n*-type NWs and metal-NP-functionalized NWs (b) with a contribution from ES, and (c) with a contribution from both ES and CS.

NWs, and a and g represent the absence and the presence of the target gas. From Eqs. (3) and (4), $(\Delta A_c)_f > \Delta A_c$ and $\left(A_g\right)_f < A_g$. Therefore, $S_e > S_p$, showing that ES by metal NPs produces a more pronounced change in the resistance of NWs. In other words, the change in the resistance of the functionalized NWs becomes greater than that of the pure NWs by ES.

Moreover, in addition to the effect of ES, CS can occur, where metal NPs can catalytically facilitate the interaction between certain gas molecules and NWs, leading to even greater suppression or expansion of the conduction channel, resulting in additional change of the resistance of the NWs. As illustrated schematically in Fig. 3c, $\left(A_g\right)_f$ decreases and, hence, $(\Delta A_c)_f$ increases in the case of the functionalized NWs as compared to that in the pure NWs. Therefore, much larger enhancement in the total gas response of the functionalized NWs can be obtained.

3.3. Electronic sensitization

The contribution of ES, which originates from relaxation of the electron-depletion layer formed beneath the metal NPs, is dependent on the interfacial area between the NPs and the NWs. The

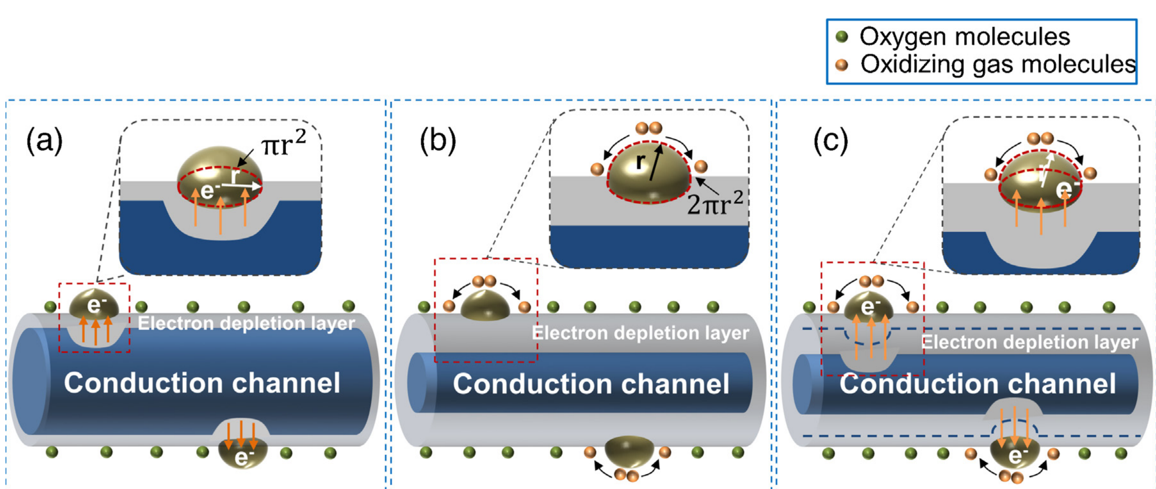

Fig. 4. Suppression of the conduction channel of NWs by (a) ES, (b) CS, and (c) both ES and CS.

transducer effect, which originates from the flow of electrons from the n-type oxide NWs to the metal NPs, is also associated with the interfacial area, and results in the suppression of the conduction channel created inside the NWs. Both the ES and transducer effects intensify the resistance change of NWs when gas molecules adsorb and desorb onto the oxide NWs. As illustrated schematically in Fig. 4a, the electron flow is likely to be proportional to the total interfacial area between the metal NPs and NWs. To simplify the model, the transducer effect is included in the ES because both can be represented by the total interfacial area.

The contribution by ES, f_{es}, per unit area of NWs, can be described using the following equation:

$$f_{es} = C_{es} \cdot \pi r^2 \cdot n \tag{5}$$

where C_{es} is a coefficient of ES, n is the number of metal NPs per unit area of NWs and r is the average radius of the attached metal NPs.

3.4. Chemical sensitization

CS is the contribution to the resistance modulation from the catalytic effect of metal NPs. This effect either facilitates the adsorption of particular gas molecules onto NWs or induces more interactions with pre-adsorbed oxygen species, which can cause the suppression or expansion of the conduction channel of the NWs, respectively. This is the source of the intensified resistance change of NWs as the gas supply is started/stopped. As shown schematically in Fig. 4b, CS is proportional to the total surface area of the attached metal NPs because the catalytic process occurs mainly on the surface of NPs. In contrast, the surface area of NWs covered by metal NPs cannot be the adsorption sites for the target gas molecules. Considering these factors, the contribution by CS, f_{cs}, per unit area of NWs, can be described as follows:

$$f_{CS} \propto \left(1 - \pi r^2 n\right)$$

$$f_{CS} \propto 2\pi r^2 .n$$

Finally, the equation becomes as follows,

$$f_{CS} = C_{CS}\left(2\pi r^2 .n\right) . \left(1 - \pi r^2 .n\right)$$

$$f_{CS} = -C_{cs} \cdot 2\pi^2 r^4 n^2 + C_{cs} \cdot 2\pi r^2 n \tag{6}$$

where C_{cs} is a coefficient of CS, and the term $\left(1 - \pi r^2 \cdot n\right)$ is associated with the decreased pristine surface area of NWs on which gas molecules can adsorb, which is due to the attachment of metal NPs and 1 represents the total area of the NWs which is unit in this case.

It is of note that the shape of the metal NPs was assumed as hemisphere because the attached NPs were generally of hemispherical shape. However, a coefficient can be included in the equations to overcome the problem originated from shape differences of the metal NPs. But since there are already coefficients in Eq. (5) and (6), it can be considered that the shape factors are also included in the coefficients C_{es} and C_{cs}. However, the trend of the equations will remain the same irrespective of the particle shape.

3.5. Total sensitization

The total contribution, f_{tot}, per unit area of NWs, by both ES and CS can be obtained by summing Eqs. (5) and (6), as follows with the assumption that only ES and CS are the prime sensitization mechanisms:

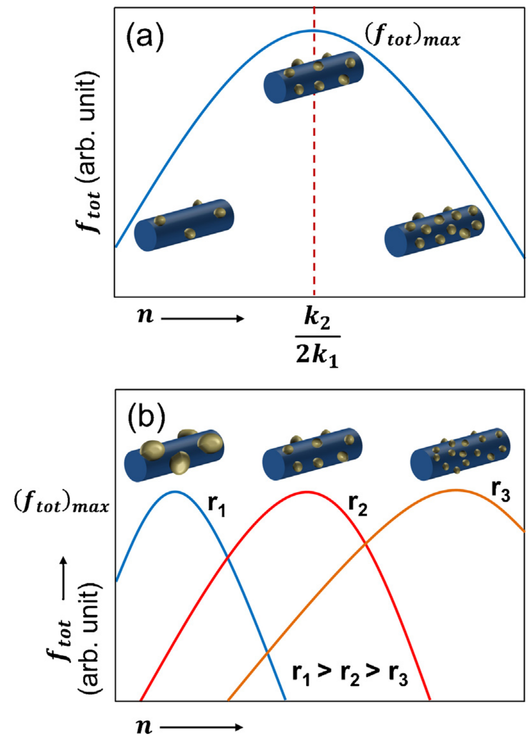

Fig. 5. Total sensitization as a function of the surface coverage of metal NPs on NWs (a) NPs of uniform size and (b) three different sizes of NPs.

The suppression of the conduction channel of NWs by both ES and CS is described in Fig. 4c. Eq. (7) shows that the total sensitization of the NWs due to the attached metal NPs greatly depends on the size r of the NPs. This value increases as the size of the NPs reduces and the amount/surface coverage n also changes accordingly. This means that the gas response of the NWs, functionalized with smaller NPs, will have greater one compared to those functionalized with larger NPs, when keeping n constant. For a fixed r, there is a certain n value at which we have maximum or optimal sensitization. This maximum value of total sensitization, $(f_{tot})_{max}$, per unit area of the NWs will be $\frac{k_2^2}{4k_1}$ at $n = \frac{k_2}{2k_1}$ for the metal NPs of a specific average radius r, as schematically shown in Fig. 5a. In other words, from Eq. (7), we can estimate the population density of the metal NPs with a certain average radius for obtaining the maximum gas response of the NWs. This sensing ability of NWs following a bell-shaped curve with regards to the amount of metal NPs functionalized is consistent with the reported literature [3,17,18,29–31] that also showed a dependence of the gas response as a function of metal NP amount. For example, Sun et al. [3] showed that a fast response and recovery in H_2S sensing could be realized using bi-functional SnO_2 NWs modulated radially with CuO NPs. An optimal amount of CuO decoration was essential for obtaining the best H_2S sensing performances of the SnO_2 NWs. Zhang et al. [29] investigated the decoration of ZnO NWs with Pt NPs that was optimized in terms of the amount of NPs for maximizing sensing efficiency. Li et al. [30] investigated the optimal amount of Pd nanocrystals coated on SnO_2 NWs to achieve the best sensing properties toward H_2S. In addition, Wongrat et al. [31] studied the ethanol sensing characteristics of ZnO-based nanostructure sensors with Au decoration applied using DC sputtering, in which the dependence of the gas sensor response on the quantity of Au coating was systematically investigated.

$$f_{tot} = f_{es} + f_{cs} = -2C_{cs}\pi^2 r^4 n^2 + \left(C_{es}\pi r^2 + 2C_{cs}\pi r^2\right) \cdot \mathrm{n} = -k_1 n^2 + k_2 \mathrm{n}; \begin{cases} k_1 = 2C_{cs}\pi^2 r^4 \\ k_2 = C_{es}\pi r^2 + 2C_{cs}\pi r^2 \end{cases} = -k_1\left(n - \frac{k_2}{2k_1}\right)^2 + \frac{k_2{}^2}{4k_1}; \quad \frac{k_2}{2k_1} = \frac{C_{es}/C_{cs} + 2}{4\pi r^2} \tag{7}$$

In addition to the case of uniform-sized metal NPs as shown in Fig. 5a, one can also predict the sensing capability of NWs with different sizes of metal NPs. Fig. 5b shows the total sensitization behaviors as a function of the surface coverage, that is population density of metal NPs, for three different sizes of metal NPs.

From Eq. (7), we can also determine the maximum value of the total sensitization as follows:

$$(f_{tot})_{max} = \left(\frac{k_2{}^2}{4k_1{}^2}\right)k_1 = \left(\frac{k_2}{2k_1}\right)^2 k_1, \text{at n} = \frac{k_2}{2k_1} = \left(\frac{\frac{C_{es}}{C_{cs}}+2}{4\pi r^2}\right)^2 \cdot \left(2C_{cs}\pi^2 r^4\right) = \frac{(C_{es}+2)^2}{8C_{cs}} = \frac{1}{2}\left(\frac{\left(C_{es}/2\right)^2 + C_{es} + C_{cs}}{C_{cs}}\right) \quad (8)$$

With Eq. (8), it is evident that the $(f_{tot})_{max}$ greatly depends on the contribution of the CS and ES due to metal NPs and that the contribution of ES to $(f_{tot})_{max}$ is greater than that of the CS. This is consistent with the reported literature [17,18,32–34] as well, and was first proposed by T. Seiyama et al. [24], in which the effects of various metal additives including Ag on SnO_2 under the influence of reducing gases were investigated. The dominant contribution of the ES to the total sensitization was ascribed to the redox reaction between Ag and Ag_2O and the consequent change in the energy band structure established at the interface between Ag/Ag_2O and SnO_2. In the presence of a reducing gas CO, the Ag^+ state is converted to Ag^0. In the presence of an oxidizing gas NO_2, the Ag^+ state is converted back to Ag^0, causing the band shift of SnO_2 and hence, the change in the (surface conductivity) resistance, which has been also confirmed by XPS analysis [18,24]. However, the values of C_{es} and C_{cs} will be significantly affected by the type of metal NPs, NWs, target gas, and the environment (temperature, humidity etc.) of the sensing chamber. Therefore, further investigations are necessary to quantify C_{es} and C_{cs}.

The phenomenological model presented in this study explains the experimental observations regarding the functionalization of oxide NWs with metal NPs and helps us to determine the optimization process of metal NPs. On the basis of Fig. 5a and b, which were plotted from Eqs. (7) and (8), the following guidelines can be addressed. First, the curve in Fig. 5a shows the bell-shaped sensing properties as a function of the amount of functionalized metal NPs with a fixed average size. That is, the optimization of the amount of metal NPs is required to have the sensor show the best sensing performance. Second, according to Fig. 5b, by decreasing the size of the NPs, the curves shift toward the right side. This indicates the population density of NPs required to obtain the maximum sensitivity must increase. That is, more NPs per unit surface area of NWs need to be decorated as the size of NPs decreases. Singh et al. [35] reported that increasing the size of Au NPs and reducing their density on the surface of the metal oxide grains and NWs, the sensor response was significantly reduced. Third, for larger-sized NPs, the width of the curve becomes narrower compared to the case of smaller-sized NPs, as shown in Fig. 5b. This suggests that more deliberate adjustment for the amount of NPs is necessary when larger-sized NPs are functionalized. Fourth, for a densely-populated metal NPs on the NWs, smaller-sized NPs will give higher sensitization in comparison to the case of larger-sized NPs. The converse will be applied for the case of dilute-populated NPs. However, it is difficult to control the population density and the size of metal NPs simultaneously. The guidelines are useful only in determination of the optimal concentration or surface density for a fixed-size metal NPs on the oxide surface as explained in the description for Eq. (7). The optimal population density of the metal NPs also depends on the surface morphology and crystallite size of oxide NWs [36–38]. Although further investigations are needed in order to quantify the exact values of C_{es} and C_{cs}, the present phenomenological model still provides us with the above-mentioned guidelines that may be useful to the optimization of metal NPs.

4. Conclusions

A model was proposed for predicting the sensing behavior of functionalized NWs in terms of the amount/surface coverage of metal NPs. This model was based on a simple geometrical consideration of metal NPs in terms of both ES and CS. Although, several assumptions have been made to simplify the model (such as the shape of NPs and NWs, type of target gas and the type of semiconducting material), the model is in good agreement with the experimental observations reported in the literature. This model provides guidelines for the functionalization of NWs with an optimal amount of metal NPs for the development of highly sensitive and selective gas sensors and can be extended to investigate the effects of other complex systems.

Acknowledgment

This study was supported by Inha University research grant.

References

[1] J.Y. Park, D.E. Song, S.S. Kim, An approach to fabricating chemical sensors based on ZnO nanorod arrays, Nanotechnology 19 (2008) 105503–105508, http://dx.doi.org/10.1088/0957-4484/19/10/105503.

[2] L.F. Zhu, J.C. She, J.Y. Luo, S.Z. Deng, J. Chen, X.W. Ji, et al., Self-heated hydrogen gas sensors based on Pt-coated $W_{18}O_{49}$ nanowire networks with high sensitivity, good selectivity and low power consumption, Sens. Actuator B—Chem. 153 (2011) 354–360, http://dx.doi.org/10.1016/j.snb.2010.10.047.

[3] G.J. Sun, S.W. Choi, A. Katoch, P. Wu, S.S. Kim, Bi-functional mechanism of H_2S detection using CuO-SnO_2 nanowires, J. Mater. Chem. C 1 (2013) 5454–5462, http://dx.doi.org/10.1039/C3tc30987h.

[4] W.C. Tian, Y.H. Ho, C.H. Chen, C.Y. Kuo, Sensing performance of precisely ordered TiO_2 nanowire gas sensors fabricated by electron-beam lithography, Sensors 13 (2013) 865–874, http://dx.doi.org/10.3390/s130100865.

[5] J. Zhang, E. Strelcov, A. Kolmakov, Heat dissipation from suspended self-heated nanowires: gas sensor prospective, Nanotechnology 24 (2013) 444009–444017, http://dx.doi.org/10.1088/0957-4484/24/44/444009.

[6] J.Y. Park, S.W. Choi, S.S. Kim, A synthesis and sensing application of hollow ZnO nanofibers with uniform wall thicknesses grown using polymer templates, Nanotechnology 21 (2010) 475601–475610, http://dx.doi.org/10.1088/0957-4484/21/47/475601.

[7] A. Katoch, S.W. Choi, G.J. Sun, S.S. Kim, Pt nanoparticle-decorated ZnO nanowire sensors for detecting benzene at room temperature, J. Nanosci. Nanotechnol. 13 (2013) 7097–7099, http://dx.doi.org/10.1166/jnn.2013.7695.

[8] S.W. Choi, A. Katoch, G.J. Sun, P. Wu, S.S. Kim, NO_2-sensing performance of SnO_2 microrods by functionalization of Ag nanoparticles, J. Mater. Chem. C 1 (2013) 2834–2841, http://dx.doi.org/10.1039/C3tc00602f.

[9] D. Meng, T. Yamazaki, T. Kikuta, Preparation and gas sensing properties of undoped and Pd-doped TiO_2 nanowires, Sens. Actuator B—Chem. 190 (2014) 838–843, http://dx.doi.org/10.1016/j.snb.2013.09.015.

[10] Q. Xiang, G. Meng, Y. Zhang, J. Xu, P. Xu, Q. Pan, et al., Ag nanoparticle embedded-ZnO nanorods synthesized via a photochemical method and its gas-sensing properties, Sens. Actuator B—Chem. 143 (2010) 635–640, http://dx.doi.org/10.1016/j.snb.2009.10.007.

[11] M. Yuasa, T. Masaki, T. Kida, K. Shimanoe, N. Yamazoe, Nano-sized PdO loaded SnO_2 nanoparticles by reverse micelle method for highly sensitive CO gas sensor, Sens. Actuator B—Chem. 136 (2009) 99–104, http://dx.doi.org/10.1016/j.snb.2008.11.022.

[12] J.K. Lung, J.C. Huang, D.C. Tien, C.Y. Liao, K.H. Tseng, T.T. Tsung, et al., Preparation of gold nanoparticles by arc discharge in water, J. Alloys Compd. 434 (2007) 655–658, http://dx.doi.org/10.1016/j.jallcom.2006.08.213.

[13] Y. Mizukoshi, S. Seino, K. Okitsu, T. Kinoshita, Y. Otome, T. Nakagawa, et al., Sonochemical preparation of composite nanoparticles of Au/(-Fe_2O_3 and magnetic separation of glutathione, Ultrason. Sonochem. 12 (2005) 191–195, http://dx.doi.org/10.1016/j.ultsonch.2003.12.003.

[14] S.-H. Choi, S.-H. Lee, Y.-M. Hwang, K.-P. Lee, H.-D. Kang, Interaction between the surface of the silver nanoparticles prepared by (-irradiation and organic molecules containing thiol group, Radiat. Phys. Chem. 67 (2003) 517–521, http://dx.doi.org/10.1016/s0969-806x(03)00097-5.

[15] S.W. Choi, S.H. Jung, S.S. Kim, Functionalization of selectively grown networked SnO_2 nanowires with Pd nanodots by gamma-ray radiolysis, Nanotechnology 22 (2011) 225501, http://dx.doi.org/10.1088/0957-4484/22/22/225501.

[16] S.S. Kim, J.Y. Park, S.W. Choi, H.S. Kim, H.G. Na, J.C. Yang, et al., Significant enhancement of the sensing characteristics of In_2O_3 nanowires by functionalization with Pt nanoparticles, Nanotechnology 21 (2010) 415502–415509, http://dx.doi.org/10.1088/0957-4484/21/41/415502.

[17] J. Ding, J.W. Zhu, P.C. Yao, J. Li, H.P. Bi, X. Wang, Synthesis of ZnO-Ag hybrids and their gas-sensing performance toward ethanol, Ind. Eng. Chem. Res. 54 (2015) 8947–8953, http://dx.doi.org/10.1021/acs.iecr.5b01711.

[18] I.S. Hwang, J.K. Choi, H.S. Woo, S.J. Kim, S.Y. Jung, T.Y. Seong, et al., Facile control of C_2H_5OH sensing characteristics by decorating discrete Ag nanoclusters on SnO_2 nanowire networks, ACS Appl Mater. Interfaces 3 (2011) 3140–3145, http://dx.doi.org/10.1021/am200647f.

[19] J.Y. Park, S.W. Choi, S.S. Kim, Junction-tuned SnO_2 nanowires and their sensing properties, J. Phys. Chem. C 115 (2011) 12774–12781, http://dx.doi.org/10.1021/Jp202113x.

[20] S.W. Choi, A. Katoch, G.J. Sun, S.S. Kim, Bimetallic Pd/Pt nanoparticle-functionalized SnO_2 nanowires for fast response and recovery to NO_2, Sens. Actuator B—Chem. 181 (2013) 446–453, http://dx.doi.org/10.1016/j.snb.2013.02.007.

[21] S.W. Choi, S.S. Kim, Room temperature CO sensing of selectively grown networked ZnO nanowires by Pd nanodot functionalization, Sens. Actuator B—Chem. 168 (2012) 8–13, http://dx.doi.org/10.1016/j.snb.2011.12.100.

[22] G.J. Sun, S.W. Choi, S.H. Jung, A. Katoch, S.S. Kim, V-groove SnO_2 nanowire sensors: fabrication and Pt-nanoparticle decoration, Nanotechnology 24 (2013) 025504–025512, http://dx.doi.org/10.1088/0957-4484/24/2/025504.

[23] N. Yamazoe, G. Sakai, K. Shimanoe, Oxide semiconductor gas sensors, Catal. Surv. Asia 7 (2003) 63–75, http://dx.doi.org/10.1023/A:1023436725457.

[24] N. Yamazoe, Y. Kurokawa, T. Seiyama, Effects of additives on semiconductor gas sensors, Sens. Actuator B—Chem. 4 (1983) 283–289, http://dx.doi.org/10.1016/0250-6874(83)85034-3.

[25] S. Matsushima, Y. Teraoka, N. Miura, N. Yamazoe, Electronic interaction between metal additives and tin dioxide in tin dioxide-based gas sensors, Jpn. J. Appl. Phys. 27 (1988) 1798–1802, http://dx.doi.org/10.1143/jjap.27.1798.

[26] L. Wang, S. Wang, M. Xu, X. Hu, H. Zhang, Y. Wang, et al., A Au-functionalized ZnO nanowire gas sensor for detection of benzene and toluene, Phys. Chem. Chem. Phys. 15 (2013) 17179–17186, http://dx.doi.org/10.1039/c3cp52392f.

[27] J.L. Freeouf, J.M. Woodall, Schottky barriers: an effective work function model, Appl. Phys. Lett. 39 (1981) 727–729, http://dx.doi.org/10.1063/1.92863.

[28] V.P. Zhdanov, nm-sized metal particles on a semiconductor surface, Schottky model, etc, Surf. Sci. 512 (2002) L331–L334, http://dx.doi.org/10.1016/S0039-6028(02)01686-2.

[29] Y. Zhang, J. Xu, P. Xu, Y. Zhu, X. Chen, W. Yu, Decoration of ZnO nanowires with Pt nanoparticles and their improved gas sensing and photocatalytic performance, Nanotechnology 21 (2010) 285501–285508, http://dx.doi.org/10.1088/0957-4484/21/28/285501.

[30] H. Li, J. Xu, Y. Zhu, X. Chen, Q. Xiang, Enhanced gas sensing by assembling Pd nanoparticles onto the surface of SnO_2 nanowires, Talanta 82 (2010) 458–463, http://dx.doi.org/10.1016/j.talanta.2010.04.053.

[31] E. Wongrat, N. Hongsith, D. Wongratanaphisan, A. Gardchareon, S. Choopun, Control of depletion layer width via amount of AuNPs for sensor response enhancement in ZnO nanostructure sensor, Sens. Actuator B—Chem. 171–172 (2012) 230–237, http://dx.doi.org/10.1016/j.snb.2012.03.050.

[32] M.S. Tong, G.R. Dai, Y.D. Wu, D.S. Gao, High sensitivity and switching-like response behavior of SnO_2-Ag-SnO_2 element to H_2S at room temperature, J. Mater. Sci.: Mater. Electron. 11 (2000) 661–665, http://dx.doi.org/10.1023/a:1008962323104.

[33] C. Dong, X. Liu, B. Han, S. Deng, X. Xiao, Y. Wang, Nonaqueous synthesis of Ag-functionalized In_2O_3/ZnO nanocomposites for highly sensitive formaldehyde sensor, Sens. Actuator B—Chem. 224 (2016) 193–200, http://dx.doi.org/10.1016/j.snb.2015.09.107.

[34] A. Gonzalezelipe, J. Soria, G. Munuera, Electron exchange in TiO_2-supported silver catalysts: I. Effect of the reducing pretreatments, J. Catal. 76 (1982) 254–264, http://dx.doi.org/10.1016/0021-9517(82)90256-1.

[35] N. Singh, R.K. Gupta, P.S. Lee, Gold-nanoparticle-functionalized In_2O_3 nanowires as CO gas sensors with a significant enhancement in response, ACS Appl. Mater. Interfaces 3 (2011) 2246–2252, http://dx.doi.org/10.1021/am101259t.

[36] G. Korotcenkov, V. Brinzari, B.K. Cho, Conductometric gas sensors based on metal oxides modified with gold nanoparticles: a review, Microchim. Acta 183 (2016) 1033–1054, http://dx.doi.org/10.1007/s00604-015-1741-z.

[37] T. Kobayashi, M. Haruta, H. Sano, M. Nakane, A selective CO sensor using Ti-doped α-Fe_2O_3 with coprecipitated ultrafine particles of gold, Sens. Actuators 13 (1988) 339–349, http://dx.doi.org/10.1016/0250-6874(88)80047-7.

[38] G. Korotcenkov, V. Brinzari, L.B. Gulina, B.K. Cho, The influence of gold nanoparticles on the conductivity response of SnO_2-based thin film gas sensors, Appl. Surf. Sci. 353 (2015) 793–803, http://dx.doi.org/10.1016/j.apsusc.2015.06.192.

Biographies

Zain Ul Abideen was born in 1990 in Attock, Pakistan. He received his B.S. in Materials Engineering from Ghulam Ishaq Khan Institute of Engineering Sciences and Technology (GIK Institute), Pakistan in June 2014. He is currently a graduate student pursuing his research at Inha University, South Korea under the supervision of Professor Sang Sub Kim since September 2014. His research interests focus on the synthesis of composite nanomaterials, metal oxide based semiconductors and their applications in chemical sensors.

Jae-Hun Kim received his B.S. degree from Gyeongsang National University, Republic of Korea in 2013. In February 2015, he received M.S. degree from Inha University, Republic of Korea. He is now working as a Ph. D. candidate at Inha University, Republic of Korea. He has been working on oxide nanowire gas sensors.

Sang Sub Kim joined the School of Materials Science and Engineering, Inha University, in 2007 as a full professor. He received his B.S. degree from Seoul National University and his M.S and Ph.D. degrees from Pohang University of Science and Technology (POSTECH) in Material Science and Engineering in 1987, 1990, and 1994, respectively. He was a visiting researcher at National Research in Inorganic Materials (currently NIMS), Japan for 2 years each in 1995 and in 2000. In 2006, he was a visiting professor at Department of Chemistry, University of Alberta, Canada. In 2010, he also served as a cooperative professor at Nagaoka University of Technology, Japan. His research interests include the synthesis and applications of nanomaterials such as nanowires and nanofibers, functional thin films, and surface and interfacial characterizations.